Development 127, 921-932 (2000)
Printed in Great Britain © The Company of Biologists Limited 2000
DEV3140

Nodal signaling patterns the organizer

Kira Gritsman, William S. Talbot* and Alexander F. Schier‡

Developmental Genetics Program, Skirball Institute of Biomolecular Medicine, Department of Cell Biology, New York University School of Medicine, 540 First Avenue, New York, NY 10016, USA

*Present address: Department of Developmental Biology, Stanford University School of Medicine, Stanford, CA 94305, USA

‡Author for correspondence (e-mail: schier@saturn.med.nyu.edu)

Accepted 15 December 1999; published on WWW 8 February 2000

SUMMARY

Spemann's organizer plays an essential role in patterning the vertebrate embryo. During gastrulation, organizer cells involute and form the prechordal plate anteriorly and the notochord more posteriorly. The fate mapping and gene expression analyses in zebrafish presented in this study reveal that this anteroposterior polarity is already initiated in the organizer before gastrulation. Prechordal plate progenitors reside close to the blastoderm margin and express the homeobox gene *goosecoid*, whereas notochord precursors are located further from the margin and express the homeobox gene *floating head*. The *nodal*-related genes *cyclops* and *squint* are expressed at the blastoderm margin and are required for prechordal plate and notochord formation. We show that differential activation of the Nodal signaling pathway is essential in establishing anteroposterior pattern in the organizer. First, overexpression of *cyclops* and *squint* at different doses leads to the induction of *floating head* at low doses and the induction of both *goosecoid* and *floating head* at higher doses. Second, decreasing Nodal signaling using different concentrations of the antagonist Antivin inhibits *goosecoid* expression at low doses and blocks expression of both *goosecoid* and *floating head* at higher doses. Third, attenuation of Nodal signaling in zygotic mutants for the EGF-CFC gene *one-eyed pinhead*, an essential cofactor for Nodal signaling, leads to the loss of *goosecoid* expression and expansion of *floating head* expression in the organizer. Concomitantly, cells normally fated to become prechordal plate are transformed into notochord progenitors. Finally, activation of Nodal signaling at different times suggests that prechordal plate specification requires sustained Nodal signaling, whereas transient signaling is sufficient for notochord development. Together, these results indicate that differential Nodal signaling patterns the organizer before gastrulation, with the highest level of activity required for anterior fates and lower activity essential for posterior fates.

Key words: Nodal, Signalling, Organizer, Pattern, *Xenopus*

INTRODUCTION

Spemann's organizer, which resides on the dorsal side of the vertebrate gastrula, has the ability to induce a secondary axis when transplanted to the ventral side of a host embryo. Organizer cells also contribute to the dorsal mesoderm of the axial midline. This axial mesoderm is regionalized along the anteroposterior axis, with the prechordal plate located anteriorly and the notochord forming more posteriorly (Spemann and Mangold, 1924; Harland and Gerhart, 1997; Schier and Talbot, 1998). Both the prechordal plate and the notochord have important roles in patterning surrounding structures such as the somites and the overlying neural plate. The prechordal plate later differentiates into head and eye muscles, pharyngeal endoderm and the hatching gland in fish (Adelmann, 1932; Keller, 1976; Jacob et al., 1984; Wachtler et al., 1984; Thisse et al., 1994; Kimmel et al., 1995), whereas the notochord is a mesodermal rod, which provides structural support to the embryo and later contributes to the development of vertebral bodies.

In the zebrafish and *Xenopus* blastula, notochord and prechordal plate precursors are both located in the dorsal equatorial region (Keller, 1976; Kimmel et al., 1990; Vodicka and Gerhart, 1995; Melby et al., 1996; Shih and Fraser, 1996; Zoltiewics and Gerhart, 1997; Harland and Gerhart, 1997; Warga and Nüsslein-Volhard, 1999). During early gastrula stages, anteroposterior polarity is already apparent, with prechordal plate progenitors located in the anterior portion of the involuting axial mesoderm and notochord precursors located more posteriorly (Keller, 1976; Melby et al., 1996; Vodicka and Gerhart, 1995; Zoltiewics and Gerhart, 1997; Harland and Gerhart, 1997). At these stages, anterior and posterior regions of the organizer also have different specification profiles, distinct inductive activities and express different marker genes (Vodicka and Gerhart, 1995; Melby et al., 1996; Zoltiewics and Gerhart, 1997; Harland and Gerhart, 1997). For instance, the expression of the homeobox genes *goosecoid (gsc)* (Cho et al., 1991; Stachel et al., 1993) and *floating head (flh)* (Talbot et al., 1995), the zebrafish homologue of *Xnot* (von Dassow et al., 1993), marks

prechordal plate progenitors and notochord progenitors, respectively (Melby et al., 1996; Cho et al., 1991; Stachel et al., 1993; Talbot et al., 1995). These observations suggest that the notochord and prechordal plate are specified before the end of gastrulation. It has not been determined, however, whether the segregation of these fates is initiated at blastula stages, or if cells become allocated to separate territories only during gastrulation.

Development of the notochord and prechordal plate requires the Nodal family of TGFβ ligands (Conlon et al.,1994; Zhou et al., 1993; Feldman et al., 1998; Sampath et al., 1998; Rebagliati et al., 1998b; reviewed in Schier and Shen, 2000). Double mutants for the zebrafish *nodal*-related genes *cyclops (cyc)* and *squint (sqt*) lack all axial mesoderm (Feldman et al., 1998). Similarly, maternal-zygotic mutants for the EGF-CFC gene *one-eyed pinhead (oep)* are missing the notochord and prechordal plate (Zhang et al., 1998; Gritsman et al., 1999). Oep is an essential cofactor for Nodal signaling in all processes thought to involve Nodal signals, including germ layer formation, floor plate development and left-right patterning (Schier et al., 1997; Gritsman et al., 1999; Yan et al., 1999). In addition, members of the Lefty family of divergent TGFβ factors, such as zebrafish Antivin (Thisse and Thisse, 1999; also called Lefty 1 (Bisgrove et al., 1999)) antagonize Nodal signaling (Meno et al., 1999; Bisgrove et al., 1999). Overexpression of Antivin can inhibit axial mesoderm formation, resulting in a phenotype that closely resembles that of *cyc;sqt* and maternal-zygotic *oep* mutants (Thisse and Thisse, 1999; Meno et al., 1999; Bisgrove et al., 1999). Together, these results suggest that Nodal signals and Oep promote axial mesoderm formation, while Lefty antagonizes it.

While Nodal signaling is required for the development of all axial mesoderm, three observations suggested that it might also be involved in specifying the difference between prechordal plate and notochord fates. First, *nodal*-related genes have a dose-dependent effect on the induction of dorsal mesodermal genes in *Xenopus* animal caps. Low levels of Nodal signaling induce the posterior mesoderm and notochord marker *Xbra*, while higher levels are needed to induce the anterior mesodermal marker *gsc* (Jones et al., 1995; Lustig et al., 1996; Erter et al., 1998). Second, zygotic *oep* mutants, which have attenuated Nodal signaling, develop a notochord but not a prechordal plate (Schier et al., 1997). Third, a partial block of Nodal signaling by overexpression of Antivin can result in a phenotype similar to that of zygotic *oep* mutants (Thisse and Thisse, 1999). Based on these results, we hypothesized that different levels of Nodal signaling regionalize the axial mesoderm during blastula or gastrula stages. Using a combination of fate mapping, marker gene expression analysis and modulation of Nodal signaling, we show here that differential Nodal signaling patterns the organizer before the onset of gastrulation, leading to the formation of prechordal plate anteriorly and notochord more posteriorly.

MATERIALS AND METHODS

Fate mapping

Fate mapping using caged fluorescein-dextran was performed as previously described in *Drosophila* (Vincent and O'Farrell, 1992) and zebrafish (Serbedzija et al., 1998; Kozlowski et al., 1997). DMNB-caged biotinylated lysine-fixable fluorescein dextran dye (Molecular Probes) was dissolved at 2.5% in 5 mg/ml Phenol red in 0.2 M KCl and centrifuged for 5 minutes. The supernatant was microinjected into embryos (0.1-0.3 nl per embryo) from an *oep^{tz57}* heterozygous intercross at the 1- to 4-cell stage. Embryos were staged according to Kimmel et al. (1995). At blastula stages, embryos were mounted in 3% methylcellulose. Uncaging was performed with a 10 second pulse of a 375 nm pulsed nitrogen laser (MicroPoint Laser System, Photonic Instruments) focused through the 40× water-immersion objective of a Zeiss Axioplan 2 microscope onto a single cell at a time. Fluorescent and Nomarski images were acquired sequentially using a cooled CCD camera (Pentamax, Princeton Instruments) and shutters (Uniblitz) controlled by the Metamorph 3.0 Imaging System (Universal Imaging). Corresponding fluorescence and Nomarski images were individually adjusted for optimal brightness and contrast and then overlayed.

The dorsoventral position of labeled cells was assigned at the onset of gastrulation, when the thickening of the shield on the dorsal side demarcates the organizer (Kimmel et al., 1990). For dorsal clones, fates were determined at tailbud stage, when the prechordal plate has the morphology of a knob formed by the most anterior hypoblast (Xu et al., 1994) and the notochord forms a thin rod just posterior to it. Fates were confirmed at 24 hours and 5 days postfertilization by fluorescence and by anti-fluorescein antibody staining as follows. Embryos were fixed in 4% paraformaldehyde in PBS at 4°C for 1 day, rehydrated in a graded series of methanol and PBT (PBS + 0.1% Tween 20), and blocked for 1 hour in 2 mg/ml BSA and 5% sheep serum in PBT at room temperature. Embryos were heat treated at 65°C for 10 minutes in blocking solution and incubated for 2 hours at room temperature with preadsorbed anti-fluorescein alkaline phosphatase Fab fragments (Boehringer Mannheim) at 1:2000 dilution in 2 mg/ml BSA in PBT. After eight 15-minute washes at room temperature, embryos were pre-equilibrated with three 5-minute washes with NTMT (0.1 M Tris-HCl pH 9.5, 50 mM $MgCl_2$, 0.1 M NaCl, 0.1% Tween 20) and stained with the NBT-BCIP substrate (Boehringer Mannheim).

Whole-mount in situ hybridization

The following plasmids were linearized and antisense RNA was synthesized by in vitro transcription: pBS*gsc* (*Eco*RI, T7; Stachel et al., 1993), pBS*flh* (*Eco*RI, T7; Talbot et al., 1995), pCS2+*sqt* (*Eco*RI, T7; Feldman et al., 1998) and pBS*cyclops* (*Not*I, T7; Rebagliati et al., 1998b). In situ hybridization with a single probe was performed as described (Schier et al., 1997) using the NBT-BCIP substrate (Boehringer Mannheim). Bicolor in situ hybridization was performed as described in Jowett and Yan (1996). The *gsc*-digoxigenin and *flh*-fluorescein probes were added to the hybridization mix simultaneously. The *flh* probe was detected using the anti-fluorescein-AP Fab fragments and developed with the NBT-BCIP substrate. After inactivation of the alkaline phosphatase, the *gsc* probe was detected with the anti-digoxigenin-AP Fab fragments and developed with the INT-BCIP substrate (Boehringer Mannheim). More background staining was observed when INT-BCIP was used as a substrate. Embryos were mounted in glycerol.

Sectioning

For plastic sections, embryos from an *oep^{tz57}* heterozygous intercross were first processed by whole-mount bicolor in situ hybridization or by hybridization with the *gsc* probe alone, and mutant embryos were identified by the absence of *gsc* expression. Stained embryos were dehydrated in a graded series of ethanol, which dissolves the INT-BCIP substrate, and embedded in Polybed resin (Ted Pella, Inc.) in trapezoid molds (Pelco, Inc.). 5 μm sagittal sections were cut on a Leica Ultracut UCT microtome.

RNA injections

The following plasmids were linearized and sense capped mRNA was

synthesized using the mMESSAGE mMACHINE system (Ambion): pcDNA3*oep*^{m134} (*Not*I, T7; Zhang et al., 1998), pCS2+*sqt* (*Not*I, SP6; Feldman et al., 1998), pCS2+*cyc* (*Not*I, SP6; Rebagliati et al., 1998), pCS2+*lacZ* (*Not*I, SP6), or pCS2+*antivin* (*Not*I, SP6; Thisse and Thisse, 1999). In vitro synthesized mRNA was injected into the yolk of 1- to 8-cell-stage wild-type embryos and embryos were fixed at 50% epiboly. For *oep*^{m134} injections, 100 pg of mRNA was microinjected into the yolk syncitial layer (YSL) of embryos from an *oep*^{tz57} homozygous intercross at blastula stages. Embryos were phenotypically analyzed and documented at 24-30 hours after fertilization. Genotyping was not required, as 100% of the progeny were maternal-zygotic *oep* mutants.

RESULTS

Fate domains for the prechordal plate and notochord in the late blastula

To determine when distinct fate domains arise for the prechordal plate and notochord, we performed fate mapping in wild-type blastulae. 1- to 4-cell-stage embryos were filled with caged fluorescein-dextran dye and left to develop to blastula stage when distinct cellular tiers are discernible from vegetal to animal positions, with tier 1 corresponding to the first row of cells at the blastoderm margin and tiers 2 and higher residing further from the margin.

We labelled rows of 15-20 cells within two tiers by laser-assisted uncaging and monitored their position and fate at later stages. We found that at dome stage (about 90 minutes before gastrulation) and 30% epiboly (about 60 minutes before gastrulation), both prechordal plate and notochord precursors can be found at the dorsal margin (data not shown). In contrast, distinct fate domains for the prechordal plate and notochord become apparent at 40% epiboly (about 45 minutes before gastrulation; Table 1, Fig. 1). Prechordal plate, but not trunk notochord, cells arise from tiers 1-2, and are later found in the hatching gland, head mesoderm and pharyngeal endoderm (Table 1; Fig. 1A-F). In contrast, notochord but not prechordal plate cells arise from tiers 6 and above (Table 1; Fig. 1G-L). Both prechordal plate and notochord cells can arise from tiers 3-5 (Table 1). When tiers 6 and above were labeled, cells began to contribute to neural fates as well as to the notochord, suggesting that the mesodermal-neural boundary in our fate map is located around the level of tier 6 (Table 1, Fig. 1L). Our data indicate that prechordal plate progenitors can be located within tiers 1-5, while notochord precursors can be found within tiers 3 and above at 40% epiboly (Table 1). These results establish that cells at the dorsal blastoderm margin become allocated to partially separate prechordal plate and notochord fate domains within the relatively short time window between dome stage and 40% epiboly.

Gsc and *flh* are expressed within subregions of the organizer

To determine how cell fates correlate with molecular specification within the organizer, we examined the expression of *gsc* and *flh*. At dome stage, both *gsc* and *flh* are expressed at the dorsal margin in cell tiers 1-5, with *flh* expression extending to tier 6 (Fig. 3C,D). In contrast, at 40% epiboly *flh* expression becomes weaker near the margin and is predominantly found within tiers 3-9 (Fig. 2C,I), while *gsc* expression is still found within tiers 1-5 (Fig. 2A,I). By 50% epiboly, *flh* is no longer expressed at the margin and is found only within tiers 3-9 (Fig. 2G,K), while *gsc* is expressed in tiers 1-5 (Fig. 2E,K). Therefore, starting at 40% epiboly, the prechordal plate fate domain overlaps with the region that expresses *gsc* and the notochord fate domain overlaps with the region that expresses *flh*. Together, these data establish that anteroposterior regionalization and fate allocation are already apparent at 40% epiboly, and thus initiated by cues operating before gastrulation.

Localized expression of *cyc* and *sqt* at the blastoderm margin

The Nodal signaling pathway has been implicated in organizer development in vertebrates (Zhou et al., 1993; Conlon et al., 1994; Feldman et al., 1998; Sampath et al., 1998; Rebagliati et al., 1998; Osada and Wright, 1999; Gritsman et al., 1999; Meno et al., 1999). In particular, the *nodal*-related genes *cyc* and *sqt*, and the Nodal cofactor *oep*, are required for prechordal plate and notochord development in zebrafish (Feldman et al., 1998; Sampath et al., 1998; Rebagliati et al., 1998b; Gritsman et al., 1999). Furthermore, *cyc* and *sqt* can both induce *gsc* upon overexpression in zebrafish embryos or in *Xenopus* animal caps (Feldman et al., 1998; Rebagliati et al., 1998a; Sampath et al., 1998; Erter et al., 1998). These observations suggested that Nodal signaling might be involved in regionalization of the organizer.

Both *sqt* and *cyc* are expressed in dorsal mesodermal progenitors at blastula stages (Feldman et al., 1998; Rebagliati et al., 1998a, Erter et al., 1998; Sampath et al., 1998). To test

Table 1. Fate mapping of dorsal tiers labeled at 40% epiboly in wild-type and zygotic *oep* mutant embryos

	Wild type				Zygotic *oep*			
Dorsal tiers at 40%	Prechordal plate	Prechordal plate and notochord	Notochord	Notochord and neural fates	Prechordal plate	Prechordal plate and notochord	Notochord	Notochord and neural fates
1-2	11	0	0	0	0	0	3	0
2-3	1	0	0	0	0	0	1	0
3-4	0	2	1	0	0	0	1	0
4-5	0	2	0	0	0	0	1	0
5-6	0	0	0	6	0	0	0	5
6-7	0	0	0	1	ND	ND	ND	ND
7-8	0	0	0	2	ND	ND	ND	ND

ND, not determined. Tiers 6-7 and 7-8 were not labeled in zygotic *oep* mutant embryos. As the mediolateral extent of labeling was variable at 40% epiboly, we also found non-dorsal fates such as the heart, trunk muscle and fin mesenchyme arising from dorsolaterally labeled cells (data not shown).

whether *cyc* and *sqt* are expressed in the right place at the right time to control anteroposterior pattern at the dorsal margin, we examined their expression in wild-type embryos at dome stage, when *gsc* and *flh* expression still overlaps within tiers 1-5 (Fig. 3C,D). At this stage, *cyc* and *sqt* are only expressed within tiers 1-2 (Fig. 3A,B). By 40% epiboly, *flh* expression becomes repressed within tiers 1-2 (Fig. 2C,I), while *gsc* expression is maintained in tiers 1-5 (Fig. 2A,I). Therefore, the blastoderm margin is a local source of Nodal-related signals before the *gsc* and *flh* expression domains become distinct.

Dose-dependent induction of ectopic *flh* and *gsc* expression by *cyc* and *sqt*

It is conceivable that different levels of Nodal signaling may lead to differential regulation of *gsc* and *flh* at the dorsal margin. As a first test of this idea, we asked how different doses of exogenous *cyc* or *sqt* would affect *gsc* and *flh* expression. mRNA encoding either *cyc* or *sqt* was microinjected into wild-type embryos at the 1- to 8-cell stage, and the injected embryos were examined for expression of *gsc* and *flh* at 50% epiboly. We found that 0.05 pg of *cyc* induced ectopic expression of *flh* but not of *gsc* (Fig. 4B,E,H,K). However, at 1 pg of *cyc*, ectopic expression of both *flh* and *gsc* was induced (Fig. 4C,F,I,L). Similar results were obtained with *sqt* (data not shown). These results indicate that lower levels of Nodal signaling are sufficient to induce ectopic *flh*, while higher levels are required to induce ectopic *gsc*. The fact that overexpression of *cyc* or *sqt* shows different dose-response effects on *gsc* and *flh* expression further suggests that Nodal-related signals may play a role in anteroposterior pattern formation in the organizer.

Decreasing the level of Nodal signaling with Antivin causes a dose-dependent repression of *gsc* and *flh*

To futher understand the role of Nodal in organizer patterning, we wanted to modulate the level of Nodal signaling in vivo. Based on the dose-dependent induction of *flh* and *gsc* by different levels of Nodal signaling, we predicted that decreasing or attenuating Nodal signaling would result in the loss of *gsc* expression at intermediate levels of Nodal signaling and in the absence of *flh* expression at low levels of Nodal signaling. We used three strategies to test this prediction. First, we decreased Nodal signaling using the inhibitor Antivin. Second, we studied the effects of attenuated Nodal signaling in zygotic *oep* mutants, which can respond to Nodal early but not late. Third, in the reverse experiment, we reconstituted Nodal signaling at different time points by adding Oep to maternal-zygotic *oep* mutants at different stages.

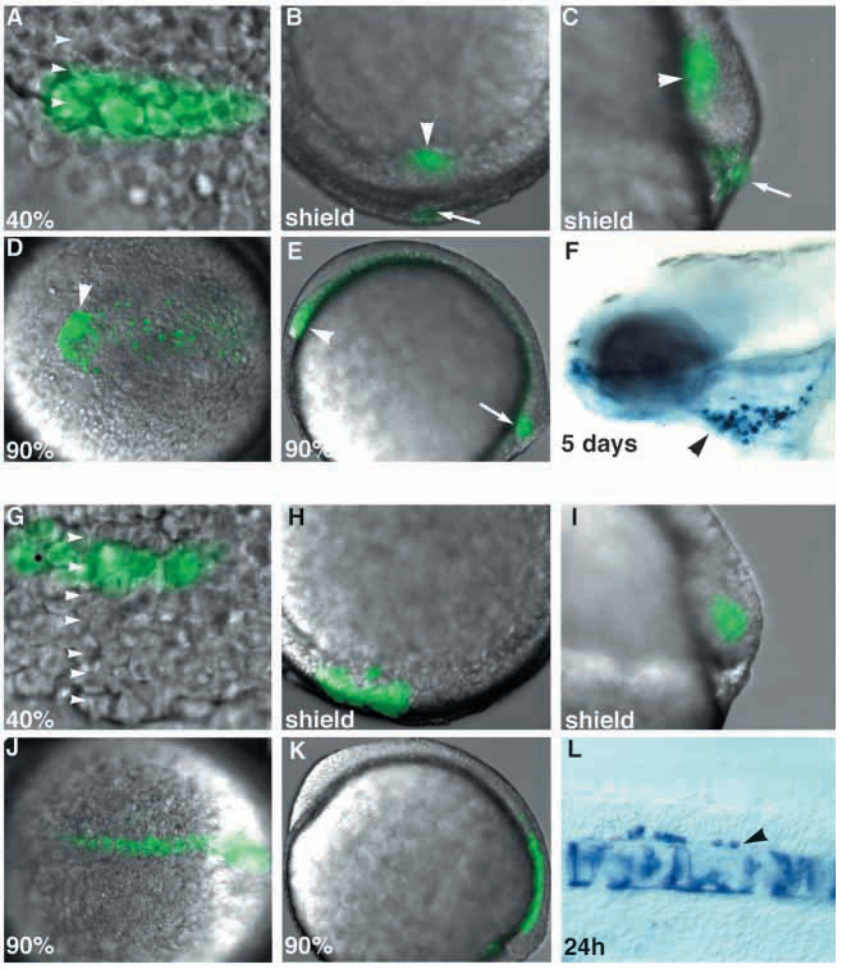

Fig. 1. Prechordal plate and notochord fate map domains in the blastula organizer. Examples of wild-type embryos labeled by uncaging at 40% epiboly (45 minutes before gastrulation). (A-F) One embryo labeled within tiers 1-2. (A) Dorsal view of the blastoderm margin, animal pole up. White arrowheads indicate cell tiers. About 15 cells within tiers 1-2 are labeled in A. (B) Animal pole view at shield stage, dorsal to the bottom. Prechordal plate precursors are in the hypoblast (white arrowhead). The other labeling is in the forerunner cells (white arrow). Forerunner cells are located within tiers 1-2 and below the margin at 40% epiboly, so they were often labeled in our experiments (Melby et al., 1996; Cooper and D'Amico, 1996). (C) Lateral view of the shield, dorsal to the right. Prechordal plate progenitors are in the hypoblast (white arrowhead). The labeled forerunner cells do not involute (white arrow). They migrate vegetally by shield stage and later contribute to tail mesoderm (arrow in E; Melby et al., 1996; Cooper and D'Amico, 1996). (D) Animal pole view of the labeled anterior prechordal plate (white arrowhead) at 90% epiboly, anterior to the left. The other labeled cells are posterior prechordal plate and/or presumptive endoderm cells that are also migrating anteriorly. (E) Lateral view at 90% epiboly, anterior to the left. Label is present in the prechordal plate (white arrowhead) and in cells of the forming tailbud (white arrow). (F) Lateral view of a 5 day old embryo stained with anti-fluorescein antibody, anterior to the left. The hatching gland (black arrowhead) and pharyngeal endoderm are labeled. (G-L) One embryo labeled within tiers 5-6. (G) Dorsal view of the blastoderm margin, animal pole up. White arrowheads indicate cell tiers. About 10 cells are labeled in tiers 5-6. (H) Animal pole view at shield stage, dorsal to the bottom. Labeled cells are still in the epiblast. (I) Lateral view of the shield, dorsal to the right. Labeled cells are in the epiblast at the boundary with the hypoblast. (J) Dorsal view at 90% epiboly, anterior to the left. (K) Lateral view at 90% epiboly, anterior to the left. Note that the posterior notochord but not the prechordal plate is labeled in J and K. (L) Lateral view of a 1 day old embryo stained with anti-fluorescein antibody, anterior to the left. The labeling is in the trunk notochord and overlying floor plate cells (black arrowhead).

In order to decrease the level of Nodal signaling, we first took advantage of Antivin, which is known to block Nodal and Activin signaling when overexpressed in zebrafish (Meno et al., 1999; Bisgrove et al., 1999; Thisse and Thisse, 1999; reviewed in Schier and Shen, 2000). To inhibit Nodal signaling to different extents, we microinjected increasing doses of *antivin* mRNA into wild-type embryos at the 1- to 8-cell stage, and then assessed *gsc* and *flh* expression at 50% epiboly. We found that decreasing Nodal signaling to intermediate levels with 2 pg of *antivin* efficiently blocks *gsc* expression, but not *flh* expression (Fig. 5B,E). In this case, *flh* is expressed ectopically in tiers 1-2 at the margin (data not shown). When Nodal signaling is decreased to very low levels with 10 pg of *antivin*, expression of both *gsc* and *flh* was inhibited (Fig. 5C,F). These results indicate that lower levels of Nodal signaling are required for *flh* expression than for *gsc* expression at the onset of gastrulation.

Posterior fate transformation of prechordal plate progenitors into notochord precursors by attenuation of Nodal signaling in zygotic *oep* mutants

As a second strategy to modulate Nodal signaling in vivo, we analyzed the phenotype of zygotic *oep* mutants. Loss of zygotic *oep* expression in the presence of maternal Oep attenuates Nodal signaling at blastula stages (Zhang et al., 1998, Gritsman et al., 1999). This results in mutants that form a notochord, but display cyclopia and lack a prechordal plate (Schier et al., 1997; Strähle et al., 1997).

To determine whether Oep functions in anteroposterior specification at the dorsal margin, we first studied the prechordal plate and notochord fate domains by analyzing marker gene expression. In zygotic *oep* mutant embryos at 40% epiboly, *gsc* expression begins to fade in intensity but occupies the same domain as in wild-type embryos (Schier et al., 1997; Fig. 2B). In contrast to wild-type embryos, however, the *flh* expression domain is expanded toward the margin in zygotic *oep* mutants, occupying tiers 1-9 (Fig. 2D,J). At 50% epiboly and at the beginning of gastrulation, *gsc* is no longer expressed in zygotic *oep* mutants (Schier et al., 1997; Fig. 2F,O), while *flh* is expressed ectopically at the margin (Fig. 2H,J,L) and in the involuting hypoblast (Fig. 2P). These results indicate that cells that normally express *gsc* and become prechordal plate in wild-type embryos express the notochord marker *flh* in zygotic *oep* mutant embryos.

To test if the attenuation of Nodal signaling in zygotic *oep* mutants might lead to the transformation of *gsc*-expressing prechordal plate precursors into *flh*-expressing notochord progenitors, we performed fate mapping in zygotic *oep* mutants at 40% epiboly (Table 1; Fig. 6). As in wild-type embryos, dorsal cells in zygotic *oep* mutants arising from tiers

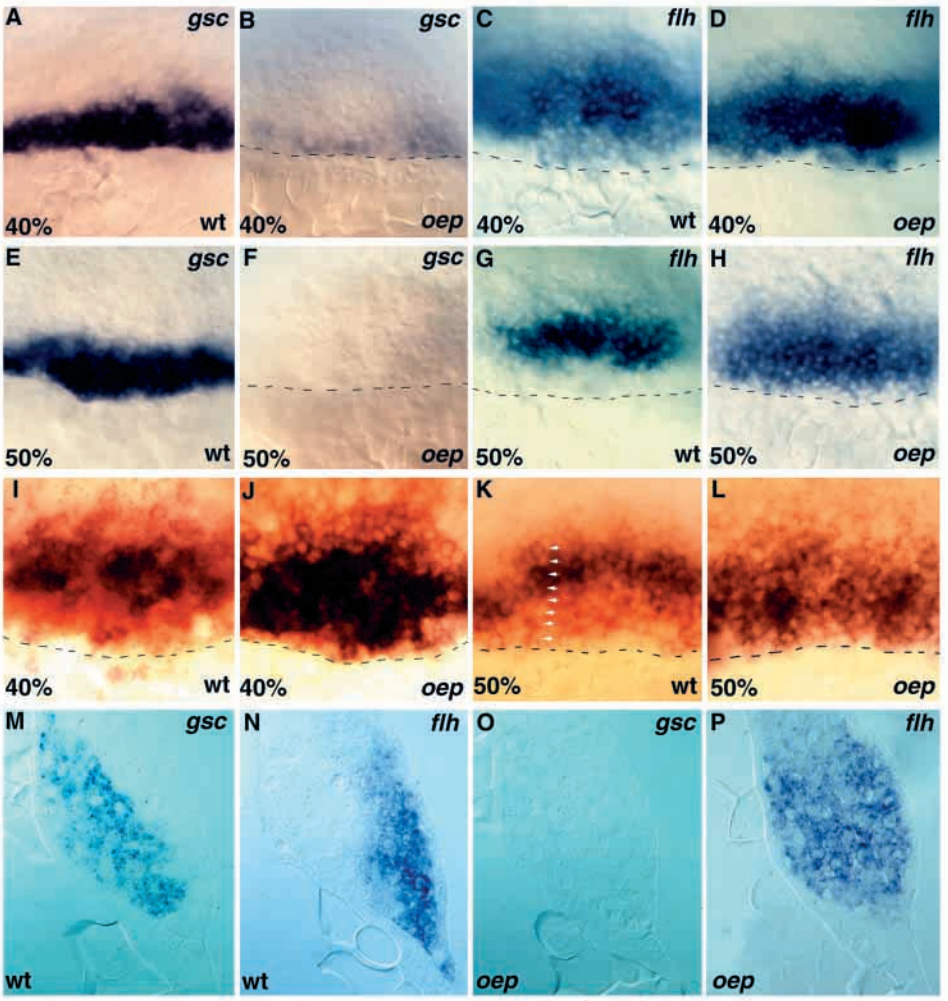

Fig. 2. Expression of *gsc* and *flh* in wild-type and zygotic *oep* mutant embryos. Whole-mount in situ hybridization was performed on wild-type and mutant embryos with *gsc* and *flh* probes. (A-L) Dorsal views of the dorsal blastoderm margin, animal pole up. *Gsc* expression in wild-type embryos at 40% epiboly (A), 50% epiboly (E) and shield stage (M). *Flh* expression in wild-type embryos at 40% epiboly (C), 50% epiboly (G) and shield stage (N). *Gsc* expression in zygotic *oep* mutant embryos at 40% epiboly (B), 50% epiboly (F) and shield stage (O). *Flh* expression in zygotic *oep* mutants at 40% epiboly (D) 50% epiboly (H) and shield stage (P). Bicolor in situ hybridization with *gsc* in orange (INT-BCIP substrate) and *flh* in black (NBT-BCIP substrate) was performed on wild-type (I,K) and zygotic *oep* mutant (J,L) embryos at 40% (I,J) and 50% (K,L) epiboly. The white arrowheads in K indicate cell tiers. Note that *flh* expression is expanded towards the margin in zygotic *oep* mutant embryos (D,H,J,L). (M-P) Lateral views of the shield, dorsal to the right. Sections were cut through the shield of wild-type (M,N) and zygotic *oep* mutant (O,P) embryos at shield stage following whole-mount in situ hybridization with *gsc* (M,O) or *flh* (N,P). Note that *gsc* expression in zygotic *oep* mutants (O) cannot be detected in the involuted hypoblast as in wild-type embryos (M). Instead, *flh* expression, which is restricted to the epiblast in wild-type embryos (N), occupies both the epiblast and the hypoblast of zygotic *oep* mutant embryos (P).

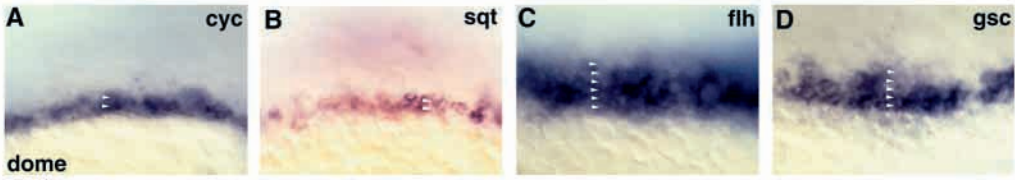

Fig. 3. Early wild-type expression of *sqt*, *cyc*, *gsc* and *flh*. Whole-mount in situ hybridization was performed on wild-type embryos at dome stage with *cyc* (A), *sqt* (B), *flh* (C) and *gsc* (D) probes. (A-D) Dorsal views of the blastoderm margin, animal pole up. White arrowheads indicate cell tiers. Note that *cyc* and *sqt* expression at dome stage is restricted to tiers 1-2. *cyc* and *sqt* continue to be expressed near the blastoderm margin until 50% epiboly (data not shown and Feldman et al., 1998; Rebagliati et al., 1998a; Erter et al., 1998).

6 and above were found in the epiblast of the early shield (Fig. 6A-C) and then contributed to the notochord (Table 1; Fig. 6D-F). Labeling within tiers 6 and above resulted in cells also adopting neural fates (Table 1; Fig. 6F), suggesting that the overall size of the region occupied by dorsal mesodermal precursors is unchanged in zygotic *oep* mutants. Similar to wild-type embryos, cells labeled in marginal tiers in zygotic *oep* mutants were present at the leading edge of the involuting hypoblast (Fig. 6G-I). However, instead of migrating anteriorly and forming a prechordal plate, these cells remained posteriorly and contributed to the notochord (Table 1; Fig. 6J-L). Cells from tiers 3-5 also contributed to the notochord (Table 1). These results establish that the organizer fate map is changed as a result of attenuation of Nodal signaling in zygotic *oep* mutant embryos. In particular, cells located in the prechordal plate domain contribute to the notochord. The failure of *oep* mutant dorsal marginal cells to adopt the correct anteroposterior pattern further supports the idea that Nodal is a key modulator of fate decisions within the presumptive organizer.

Varying the exposure times to Oep affects the response to Nodal signaling

Our analysis of zygotic *oep* mutants indicates that attenuated Nodal signaling is sufficient to specify posterior fates near the dorsal margin, but anterior fate specification requires full activation of the Nodal signaling pathway. The extent of activation of this pathway may be determined partly by the period of time that dorsal marginal cells can respond to Nodal signaling, which depends upon the availability of Oep (Gritsman et al., 1999). Our third strategy to modulate Nodal signaling in vivo was to administer Oep at different times to maternal-zygotic *oep* mutants, to enable them to respond to Nodal signaling for different durations.

We previously showed that injection of mRNA encoding the secreted version of Oep termed *oep*^{m134} (Zhang et al., 1998) can rescue maternal-zygotic *oep* mutants by injection into the extraembryonic yolk syncytial layer (YSL) at early blastula stages (Gritsman et al., 1999). To modulate the response of marginal cells to Nodal signaling, we injected *oep*^{m134} mRNA at different times into the YSL of maternal-zygotic *oep* mutants and asked how this would affect anteroposterior patterning at the dorsal margin. First, we assessed the phenotypes of live embryos at 30 hours. Only the earliest injections at oblong stage resulted in embryos with extensive rescue (class I phenotype; Fig. 8). These embryos looked almost wild type, with two eyes and a hatching gland, suggesting that the prechordal plate was rescued (Fig. 7B,G). Later injections at sphere stage (1 hour later than oblong), dome stage (2 hours later than oblong), or 30% epiboly (2.5 hours later than oblong) resulted in partially rescued embryos with class II or class III phenotypes (Fig. 8). Class II embryos had cyclopia with no hatching gland, but had rescue of the notochord and trunk muscle (Fig. 7C,H). Class III embryos had cyclopia with no hatching gland or notochord, but had rescue of the trunk somites and blood (Fig. 7D,I,E,J). The cyclopia and lack of hatching gland in class II and III embryos suggests that the prechordal plate was not rescued in these cases.

We also analyzed *gsc* and *flh* expression in similarly injected

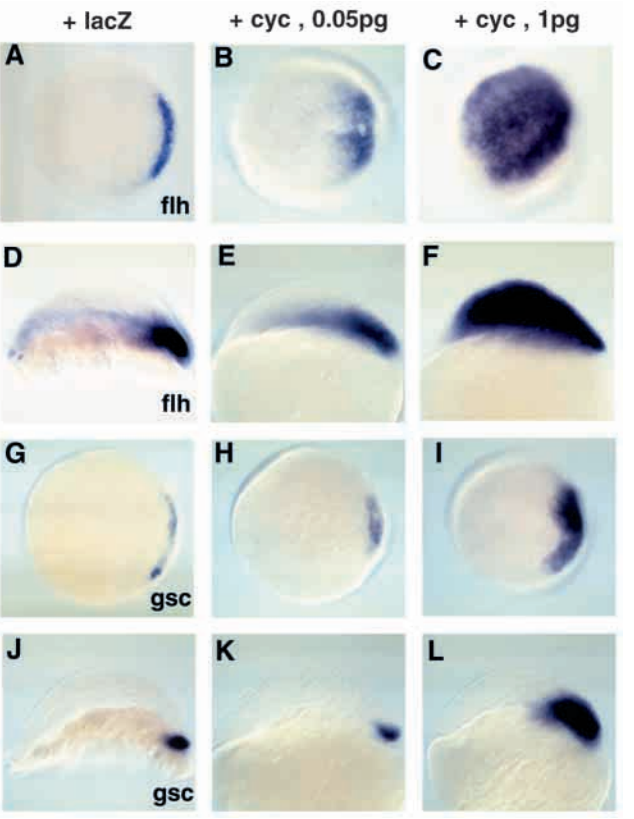

Fig. 4. Dose-dependent induction of ectopic *flh* and *gsc* by *cyc*. Wild-type embryos were microinjected at the 1- to 8-cell stage with mRNA encoding *lacZ* (A,D,G,J), or *cyc* (B,C,E,F,H,I,K,L) and *gsc* or *flh* expression was examined at 50% epiboly. (A-C, G-I) Animal pole views, dorsal to the right. (D-F, J-L) Lateral views, dorsal to the right. (A-F) *Flh* expression. (G-L) *Gsc* expression. (B,E,H,K) Embryos injected with 0.05 pg of *cyc*. 9/13 embryos had ectopic *flh* expression (B,E). 0/18 embryos had ectopic *gsc* expression (H,K). *Gsc* expression was lost in 6/18 embryos (data not shown). (C,F,I,L) Embryos injected with 1 pg of cyc. 39/39 embryos had ectopic *flh* expression (C,F). 36/37 embryos had ectopic *gsc* expression (I,L).

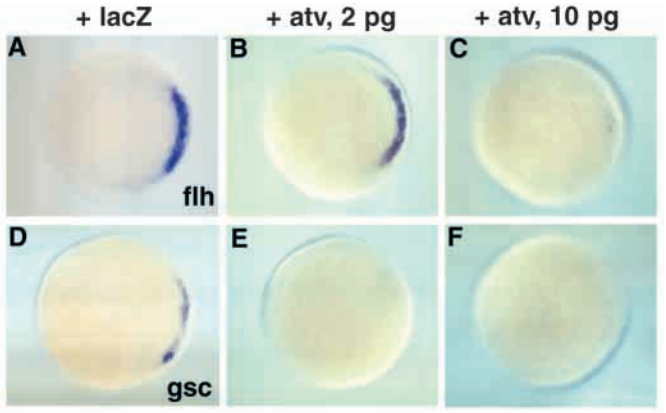

Fig. 5. Dose-dependent inhibition of *gsc* and *flh* by Antivin. Wild-type embryos were microinjected at the 1- to 8-cell stage with mRNA encoding *lacZ* (A,D) or *antivin* (B,C,E,F) and *gsc* or *flh* expression was analyzed at 50% epiboly. (A-F) Animal pole views, dorsal to the right. (A-C) *Flh* expression. (D-F) *Gsc* expression. (B,E) Embryos injected with 2 pg of *antivin*. *Flh* was expressed in 36/36 embryos (B). *Gsc* was inhibited in 18/23 embryos (E). (C,F) Embryos injected with 10 pg of *antivin*. *Flh* was inhibited in 10/19 embryos (C). *Gsc* was inhibited in 16/16 embryos (F).

maternal-zygotic *oep* embryos at 50% epiboly. Uninjected maternal-zygotic *oep* mutants do not express *gsc* (Fig. 7K) and express very reduced levels of *flh* (Fig. 7N) at 50% epiboly. The earliest injection of oep^{m134} mRNA at the 1K stage rescued *gsc* expression to levels slightly lower than wild-type levels in 13/16 embryos (Fig. 7L), and rescued *flh* in 19/20 embryos (Fig. 7O). These embryos expressed *flh* throughout tiers 1-9 (data not shown), suggesting that rescue was incomplete. Injection 1 hour later at sphere stage failed to rescue *gsc* in 18/20 embryos (Fig. 7M), but could still rescue *flh* in 14/19 embryos (Fig. 7P). In this case *flh* was also expressed throughout tiers 1-9 (data not shown). In summary, we observed more complete rescue when we injected oep^{m134} mRNA earlier, suggesting that, at the concentration we examined, sustained Nodal signaling is required for *gsc* expression and prechordal plate formation, whereas transient Nodal signaling is sufficient for *flh* expression and notochord development (Figs 7, 8).

DISCUSSION

Anteroposterior patterning of the organizer is initiated prior to gastrulation

In previous zebrafish fate maps (Kimmel et al., 1990; Shih and Fraser, 1995; Melby et al., 1996; Warga et al., 1999), the notochord and structures derived from the prechordal plate were both found to arise from the dorsal blastoderm margin, the region of the organizer. It has been unclear, however, if these two fates are already segregated before gastrulation. To locate a specific fate domain for the prechordal plate, we labeled cells before the onset of gastrulation. Fates were assigned at the end of gastrulation, when the prechordal plate is visible as a coherent structure anteriorly, and the notochord is seen more posteriorly. By labeling tiers of cells along the animal-vegetal axis at varying distances from the dorsal blastoderm margin, we were able to locate distinct but partially overlapping anterior and posterior fate domains starting at 40% epiboly, about 45 minutes before involution begins. As we never saw trunk notochord cells arising from tiers 1-2 at this stage, we can exclude the possibility that prechordal plate and notochord precursors are intermingled at the margin. Likewise, there is no intermingling between these two fates in tiers 6 and above, which contain notochord precursors but no prechordal plate precursors. There may be common progenitors for the prechordal plate and notochord within tiers 3-5, where we see an overlap between these fates. Alternatively, prechordal plate and notochord progenitors may be intermingled within this region. The overlap between these two fates within tiers 3-5 suggests that there is further refinement of the anteroposterior pattern after 40% epiboly.

The pattern that we have observed by fate mapping correlates closely with the expression of the homeobox genes *gsc* and *flh*. Current resolution does not allow us to determine overlap at the single cell level, but at 40-50% epiboly *gsc* is expressed closer to the blastoderm margin where the prechordal plate precursors are located, while *flh* is expressed farther from the margin, in the region occupied by notochord progenitors. Indeed, there might be a causal relationship between the expression of these organizer genes and the fate of cells: *flh* is an essential determinant of notochord development (Talbot et al., 1995, Halpern et al., 1995; Melby et al., 1996; Gont et al., 1996) and *gsc* can induce migratory behavior reminiscent of prechordal plate cells (Niehrs et al., 1993). Moreover, we found that *flh*-expressing cells at the margin of zygotic *oep* mutants acquire a notochord fate instead of prechordal plate fate.

In summary, our results suggest three different stages of anteroposterior pattern formation in the axial mesoderm. Initially, there is a mixed population of cells that can contribute to either prechordal plate or notochord and express both *flh* and *gsc*. Beginning at 40% epiboly, dorsal marginal cells segregate into prechordal plate and notochord fate domains and *gsc*- and *flh*-expressing regions. The complete allocation of prechordal plate and notochord cells occurs during gastrulation, resulting at the end of gastrulation in non-overlapping territories of *gsc*-expressing prechordal plate cells anteriorly and *flh*-expressing notochord cells posteriorly. Importantly, the occurrence of anteroposterior pattern prior to gastrulation demonstrates that regionalization within the organizer is an active process already initiated before gastrulation by early inductive cues, rather than a passive process enacted exclusively by gastrulation movements.

Differential Nodal signaling generates anteroposterior pattern in the organizer

Previous studies have shown that Nodal signaling is required for the development of the entire axial mesoderm (Feldman et al., 1998; Gritsman et al., 1999; Thisse and Thisse, 1999; Bisgrove et al., 1999; Meno et al., 1999). The results presented here indicate an additional role for Nodal signaling in patterning axial mesoderm precursors in the organizer along the anteroposterior axis by differential activation of the Nodal signaling pathway. This conclusion is based on three different experimental approaches to modulate Nodal signaling in vivo. First, we overexpressed Antivin/Lefty, which acts as an inhibitor of Nodal signaling, at increasing levels in wild-type embryos (Thisse and Thisse, 1999; Bisgrove et al., 1999; Meno et al., 1999). Antivin

overexpression causes cyclopia and loss of prechordal plate at low doses and eliminates all axial mesoderm at higher doses (Thisse and Thisse, 1999). We found that decreasing Nodal signaling with low doses of Antivin can abolish *gsc* expression at 50% epiboly, while higher doses of Antivin are needed to inhibit *flh* expression. These results indicate that anterior organizer fates require higher levels of Nodal signaling than posterior fates.

Second, we analyzed the fate of dorsal marginal cells in zygotic *oep* mutants, which attenuate Nodal signaling during blastula stages. We have shown that cells within the prechordal plate fate domain lack expression of *gsc*, misexpress *flh* and adopt a notochord fate. This early perturbation in marker gene expression indicates that the subsequent changes in cell migration and differentiation are likely to be a consequence of the misspecification of these marginal cells as notochord progenitors. To test the possibilty that the prechordal plate precursors are simply deleted and then replaced by notochord progenitors, we labeled cells within the notochord fate domain in zygotic *oep* mutants. We found that the notochord fate domain, as well as the boundary between mesodermal and neural progenitors, appear unchanged in zygotic *oep* mutants. These results show that zygotic *oep* mutants have the same approximate number of mesodermal progenitors as wild-type embryos, but all cells within this region express *flh* and can contribute to the notochord. Therefore, the dorsal marginal cells undergo a posterior fate transformation upon attenuation of Nodal signaling in the absence of zygotic Oep. This suggests that early Nodal signaling in zygotic *oep* mutants is sufficient for expression of *flh* at the dorsal margin and maintenance of notochord fates, but not sufficient to maintain prechordal plate fates and *gsc* expression at the margin.

Third, we modulated the activation of the Nodal signaling pathway during blastula stages by adding Oep to maternal-zygotic *oep* mutants at different times. We found that longer exposure to a given level of Oep can rescue both prechordal plate and notochord formation and both *gsc* and *flh* expression in these mutants, while shorter exposure can only rescue *flh* expression and notochord development. This result might be due to exposure to Nodal signals for different times and could also be influenced by the degree of Nodal accumulation.

Taken together, our analysis of marker gene expression and fate specification in the context of reduced Nodal signaling indicates that differential Nodal signaling is required for the specification of prechordal plate and notochord fates and for anteroposterior patterning in the organizer. In particular, our results suggest that anterior fates close to the organizer margin require high levels of Nodal signaling, whereas more posterior fates at a distance from the margin require lower levels of Nodal signaling.

Several mechanisms can generate differential Nodal signaling

How might the Nodal signaling pathway be activated

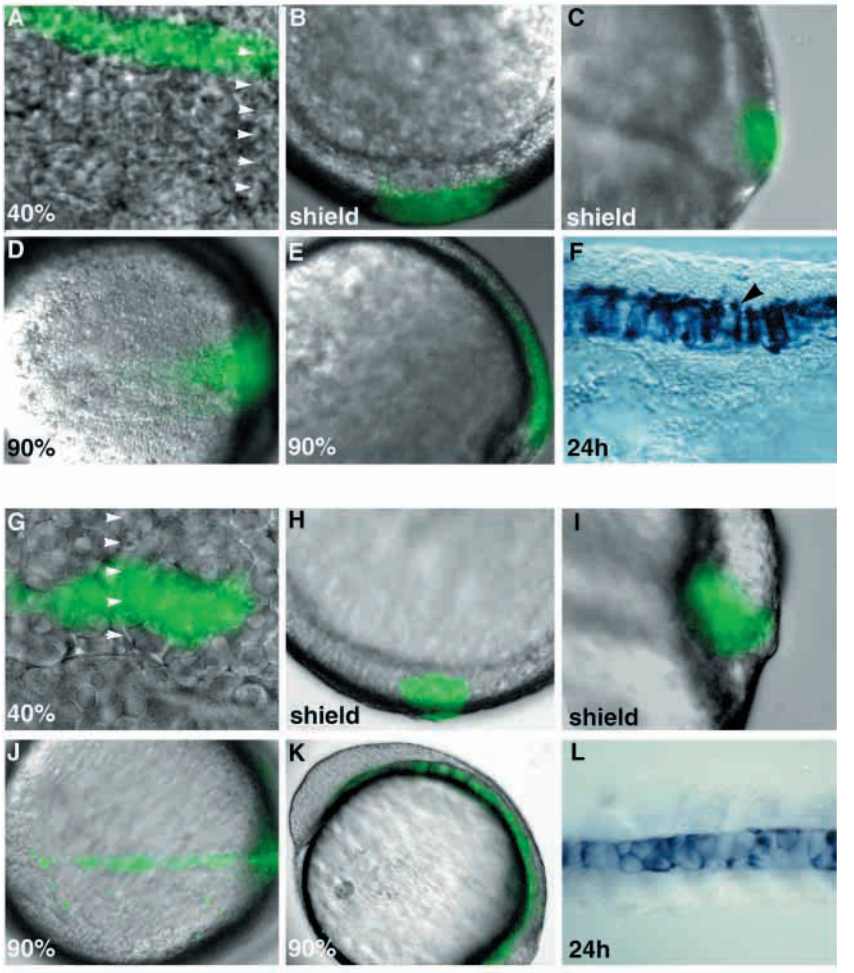

Fig. 6. Posterior transformation of the blastula organizer in zygotic *oep* mutants. Examples of zygotic *oep* mutant embryos labeled by uncaging at 40% epiboly. (A≠F) One embryo labeled within tiers 5-6. (A) Dorsal view of the blastoderm margin, animal pole up. About 20 cells are labeled. White arrowheads indicate cell tiers. (B) Animal pole view at shield stage, dorsal to the bottom. (C) Lateral view of the shield, dorsal to the right. Note that the labeled cells are in the epiblast in B and C. (D) Dorsal view at 90% epiboly, anterior to the left. (E) Lateral view at 90% epiboly, anterior up and to the left. Note that the posterior notochord is labeled in D and E. (F) 1-day-old embryos stained with the anti-fluorescein antibody. Lateral view, anterior to the left. Note that the notochord is labeled. Some overlying ventral neural tube cells are also labeled (black arrowhead). (G,H) One embryo labeled within tiers 2-3. (G) Dorsal view of the blastoderm margin, animal pole up. About 15 cells are labeled. White arrowheads indicate cell tiers. (H) Animal pole view at shield stage, dorsal to the bottom. Note that the labeled cells are in the shield. (I) Lateral view of the shield, dorsal to the right. Note that the labeled cells are in the hypoblast. (J) Dorsal view at 90% epiboly, anterior to the left. (K) Lateral view at 90% epiboly, anterior up and to the left. Note that the notochord is labeled in J and K. Note that the cells in K extend up to the anterior-most extent of the notochord, but not into the anterior head region as found in wild-type embryos labeled in tiers 2-3. (L) 1-day-old embryo stained with the anti-fluorescein antibody. Dorsal view, anterior to the left. Note the notochord labeling. No labeled cells were observed in the head region anterior to the notochord (data not shown).

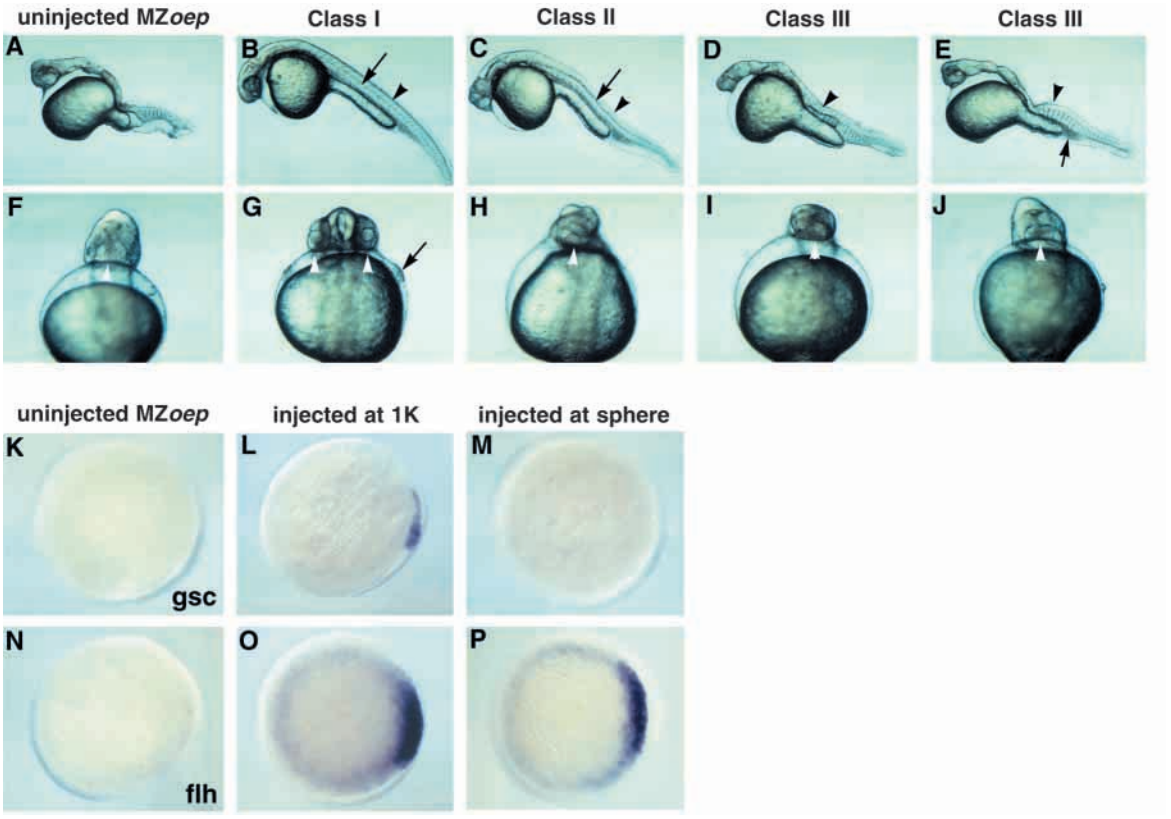

Fig. 7. Phenotypes of maternal-zygotic *oep* embryos rescued by *oep*^{m134} RNA injection. Maternal-zygotic *oep* mutant embryos were injected into the YSL with 100 pg mRNA encoding *oep*^{m134} at late blastula stages. (A-J) Live embryos at 30 hpf. (A-E) Lateral view, anterior to the left. (F-J) Ventral view, anterior up. (A,F) Uninjected maternal-zygotic *oep* embryo. (B-E,G-J) *oep*^{m134} RNA-injected embryos. (B,G) Class I embryo. Note the notochord (black arrow in B), trunk somites (black arrowhead in B), two eyes (white arrowheads in G) and hatching gland (black arrow in G). (C,H) Class II embryo. Note the notochord (black arrow in C), trunk somites (black arrowhead in C) and cyclopic eye (white arrowhead in H). Class III embryos (D,E,I,J). Note the trunk somites (black arrowhead in D,E), blood (black arrow in E) and cyclopia (white arrowhead in I,J). (K-P) In situ hybridization with *gsc* or *flh* probes was performed on maternal-zygotic *oep* embryos at 50% epiboly. Animal pole views, dorsal to the right. (L,M,O,P) Maternal-zygotic *oep* embryos injected into the YSL with 100 pg of *oep*^{m134} RNA. (K-M) *Gsc* expression. (N-P) *Flh* expression. (K,N) Uninjected maternal-zygotic *oep* embryos. (L,O) Embryos injected at 1K stage. *Gsc* was rescued in 13/16 embryos (L), while *flh* was rescued in 19/20 embryos (O). (M,P) Embryos injected at sphere stage. *Gsc* was rescued in only 2/20 embryos (M, non-rescued embryo shown), while *flh* was rescued in 14/19 embryos (P).

differentially within the organizer to generate anteroposterior pattern? Our results can be interpreted in light of recent studies on the patterning activities of the TGFβ ligand Activin. Activin has been studied extensively as an example of a morphogen that can pattern the mesoderm (Green et al., 1992, 1997; Gurdon et al., 1994, 1995, 1996, 1998; Jones et al., 1996; McDowell et al., 1997; Dyson and Gurdon, 1998). In *Xenopus* animal caps, Activin can induce *gsc* at high concentrations and *Brachyury* (*Xbra*), a marker for the notochord and posterior mesoderm, at lower concentrations (Green et al., 1997). In addition, *gsc* is induced closer to the source of Activin than *Xbra*, suggesting that Activin protein can form a gradient by diffusion (Gurdon et al., 1994). Furthermore, it has been shown that a longer period of exposure to Activin is required to induce *gsc* than *Xbra* (Gurdon et al., 1995; Dyson and Gurdon, 1998). Detailed quantitative studies have revealed that downstream gene activation depends on the absolute number of receptors occupied by Activin per cell (Dyson and Gurdon, 1998). Importantly, higher occupancy can be achieved either by exposure to a higher concentration of Activin, or by receiving a constant amount of Activin for a longer period of time (Dyson and Gurdon, 1998). While the in vivo role of Activin is unclear (Harland and Gerhart, 1997; Matzuk et al., 1995; Schulte-Merker et al., 1994), these results suggest a model wherein a localized source of a TGFβ ligand could pattern surrounding tissue in a concentration- and time-dependent fashion.

Several observations suggest that a similar mechanism may explain the cell fate decisions in response to Nodal signaling. First, Nodal-related ligands are thought to signal via a similar intracellular pathway as Activin (Oh and Li, 1997; Whitman, 1998; Waldrip et al., 1998; Weinstein et al., 1998; Nomura and Li, 1998; Gu et al., 1998; Gritsman et al., 1999; Meno et al., 1999; Song et al., 1999; reviewed in Schier and Shen, 2000). Second, ectopic expression of *nodal*-related genes can cause similar phenotypes and dose responses as Activin in *Xenopus* and zebrafish embryos (Jones et al., 1995; Joseph and Melton, 1997; Rebagliati et al., 1998a; Erter et al., 1998; Sampath et al., 1998). Third, we have shown that overexpression of the zebrafish *nodal*-related genes *cyc* and *sqt* has a dose-dependent effect on axial mesoderm markers: ectopic *flh* is induced at low levels of *cyc* or *sqt* expression, while ectopic *gsc* is induced

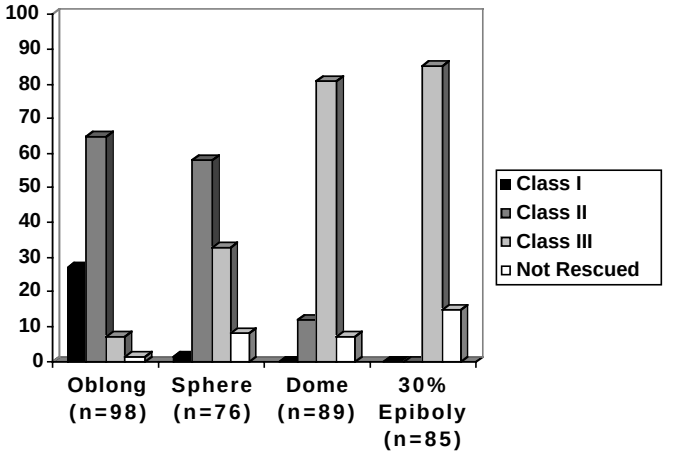

Fig. 8. Rescue of maternal-zygotic *oep* embryos by *oep*^{m134} RNA injection at different times. 100 pg of mRNA encoding *oep*^{m134} was injected at oblong stage, sphere stage (oblong +1h), dome stage (oblong +2h), or 30% epiboly (oblong +2.5h) into the YSL of maternal-zygotic *oep* mutant embryos. Phenotypes were analyzed at 30 hours. See Fig. 7 for class I, II and III phenotypes. Note that class I rescue is observed predominantly at oblong stage, while class II rescue is possible until dome stage.

only at higher levels. Fourth, *cyc* and *sqt* are both expressed at the blastoderm margin at dome stage, before the expression domains of *gsc* and *flh* become distinct. This localized expression could allow cells close to the blastoderm margin to experience higher concentrations of Nodal-related protein. In the simplest model, these results and the morphogen-like properties of Activin suggest that during normal development high levels of Nodal signals close to the margin allow expression of *gsc*, whereas lower levels in higher tiers allow for maintenance of *flh* expression. In this model, loss of Nodal signals would lead to a loss of *gsc* and *flh* expression (as observed in *cyc;sqt* mutants and maternal-zygotic *oep* mutants), whereas a decrease in Nodal signaling would block *gsc* but not *flh* expression (as observed in zygotic *oep* mutants and upon expression of low doses of Antivin).

While our results are consistent with the idea that Cyc and Sqt could act as morphogens to pattern the organizer along the anteroposterior axis, the range of action of Cyc and Sqt in vivo has yet to be determined. For instance, it has been shown that the Nodal-related protein Xnr2 can only act at short range in *Xenopus* ectodermal explants (Jones et al., 1996). It is thus still possible that the differential regulation of *gsc* and *flh* is not mediated directly by different concentrations of Nodal signals, but indirectly by relay factors that are regulated by Nodal signaling.

Interestingly, our results suggest that organizer patterning might not only be dependent on different concentrations of Nodal signals, but also on the length of exposure to these signals. In particular, the attenuation of Nodal signaling at blastula stages in zygotic *oep* mutants causes a transformation of prechordal plate precursors into notochord progenitors. Furthermore, in our partial rescue experiment using maternal-zygotic *oep* mutants, transient exposure to Nodal signaling can only rescue the notochord, while sustained exposure is required to rescue the prechordal plate. These results suggest that cell fate decisions are influenced by the duration of signaling. Consistent with this observation, different exposure times to Activin can also result in different cellular responses (Gurdon et al., 1995; Dyson and Gurdon, 1998). Furthermore, it has been shown in the case of tyrosine kinase signaling that transient versus sustained activation of this signaling pathway leads to distinct cellular responses (reviewed in Marshall, 1995). We thus propose that both Nodal activity at a given time and the time of exposure to Nodal signaling are critical for fate decisions in dorsal marginal cells. The extent of activation of the Nodal signaling pathway within a cell would thus depend upon several factors: the concentration of Nodal protein, the distance of responding cells from the source of Nodal, the length of time exposed to Nodal signals, the concentration of inhibitory proteins such as Antivin, and the availabilty of Oep. The interplay of these factors would result in high Nodal signaling close to the margin, causing specification of prechordal plate progenitors, and lower Nodal signaling in higher tiers, resulting in specification of notochord progenitors.

Role of Nodal signaling in patterning along the animal-vegetal axis

We have shown that differential Nodal signaling plays an important role in animal-vegetal patterning on the dorsal side of the embryo. In the zebrafish and *Xenopus* blastula, there is also an animal-vegetal pattern in lateral and ventral regions, with endoderm progenitors located vegetally and most mesoderm precursors located more animally (Dale and Slack, 1987; Warga and Nusslein-Volhard, 1999). In zebrafish, Nodal signaling is required for endoderm formation (Schier et al., 1997; Strahle et al., 1997; Feldman et al., 1998; Gritsman et al., 1999; Rodaway et al., 1999; Alexander and Stainier, 1999) and evidence from *Xenopus* animal cap assays suggests that higher levels of Nodal signaling are needed to induce endodermal markers than mesodermal markers (Piccolo et al., 1999; Clements et al., 1999; Yasuo and Lemaire, 1999; Erter et al., 1998; Zorn et al., 1999). Interestingly, zygotic *oep* mutants, which have attenuated Nodal signaling, form most mesoderm, but lack both prechordal plate and endoderm (Schier et al., 1997; Strähle et al., 1997). These data suggest that, similar to prechordal plate formation at the dorsal margin, high levels of Nodal signaling are essential for endoderm specification of marginal cells. Therefore, the essential role of Nodal signaling in anteroposterior patterning of the organizer may be just one example of a more general function for Nodal signaling in patterning the blastula along the animal-vegetal axis.

We thank M. Chao, J. Schlessinger, E. Skolnik, A. Whitty and the members of the Schier and Talbot laboratories for helpful discussions, B. Feldman and G. Fishell for help with fate mapping and microscopy, S. Burden, R. Burdine, Y. Chen, R. Lehmann and H. Sirotkin for comments on the manuscript, and S. McManus and R. Feeney for fish maintenance. This work was supported by NIH RO1GM57825 (W. S. T.), the Pew Scholars Program (W. S. T.) and NIH RO1GM56211 (A. F. S.). A. F. S. is a Scholar of the McKnight Endowment Fund for Neuroscience.

REFERENCES

Adelman, H. B. (1932). The development of the prechordal plate and mesoderm of Amblystoma punctatum. *J. Morph.* **54**, 1-67

Alexander, J. and Stainier, D. Y. R. (1999). A molecular pathway leading to endoderm formation in zebrafish. *Current Biol.* **9**, 1147-1157

Bisgrove, B. W., Essner, J. J. and Yost, H. J. (1999). Regulation of midline development by antagonism of *lefty* and *nodal* signaling. *Development* **126**, 3253-3262

Cho, K. W., Blumberg, B., Steinbesser, H. and DeRobertis, E. M. (1991). Molecular nature of Spemann's organizer: the role of the Xenopus homeobox gene *goosecoid*. *Cell* **67**, 1111-1120

Clements, D., Friday, R. V. and Woodland, H. R. (1999). Mode of action of VegT in mesoderm and endoderm formation. *Development* **126**, 4903-4911

Conlon, F. L., Lyons, K. M., Takaesu, N., Barth, K. S., Kispert, A., Herrmann, B. and Robertson, E. J. (1994). A primary requirement for nodal in the formation and maintenance of the primitive streak in the mouse. *Development* **120**, 1919-1928

Cooper, M. S. and D'Amico, L. A. (1996). A cluster of noninvoluting endocytic cells at the margin of the zebrafish blastoderm marks the site of embryonic shield formation. *Dev. Biol.* **180**, 184-198

Dale, L. and Slack, J. M. W. (1987). Fate map for the 32-cell stage of *Xenopus laevis*. *Development* **99**, 527-551

Dyson, S. and Gurdon, J. B. (1998). The interpretation of position in a morphogen gradient as revealed by occupancy of Activin receptors. *Cell* **93**, 557-568

Erter, C. E., Solnica-Krezel L. and Wright, C. V. E. (1998). Zebrafish *nodal-related 2* encodes an early mesendodermal inducer signaling from the extraembryonic yolk syncytial layer. *Dev. Biol.* **204**, 361-372

Feldman, B., Gates, M. A., Egan, E. S., Dougan, S. T., Rennebeck, G., Sirotkin, H. I., Schier, A. F. and Talbot, W. S. (1998). Zebrafish organizer development and germ-layer formation require nodal-related signals. *Nature* **395**, 181-185

Gont, L. K., Fainsod, A., Kim, S. H. and DeRobertis, E. M. (1996). Overexpression of the Homeobox Gene Xnot-2 Leads to Notochord Formation in *Xenopus*. *Dev. Biol.* **174**, 174-178

Green J. B. A., New, H. V. and Smith, J. C. (1992). Responses of embryonic Xenopus cells to activin and FGF are separated by multiple dose thresholds and correspond to distinct axes of the mesoderm. *Cell* **71**, 731-739

Green, J. B. A., Cook, T. L., Smith, J. C. and Grainger, R. M. (1997). Anteroposterior neural tissue specification by activin-induced mesoderm. *Proc. Natl. Acad. Sci. USA* **94**, 8596-8601

Gritsman, K., Zhang, J., Cheng, S., Heckscher, E., Talbot, W. S. and Schier, A. F. (1999). The EGF-CFC protein one-eyed pinhead is essential for nodal signaling. *Cell* **97**, 121-132

Gu, Z., Nomura, M., Simpson, B. B., Lei, H., Feijen, A., van den Eijnden-van Raaij, J., Donahoe, P. K. and Li, E. (1998). The type I activin receptor ActRIB is required for egg cylinder organization and gastrulation in the mouse. *Genes Dev.* **12**, 844-57

Gurdon, J. B., Harger, P., Mitchell, A. and Lemaire, P. (1994). Activin signalling and response to a morphogen gradient. *Nature* **371**, 487-492

Gurdon, J.B., Mitchell, A. and Mahony, D. (1995). Direct and continuous assessment by cells of their position in a morphogen gradient. *Nature* **376**, 520-521

Gurdon, J. B., Mitchell, A. and Ryan, K. (1996). An experimental system for analyzing response to a morphogen gradient. *Proc. Natl. Acad. Sci. USA* **93**, 9334-9338

Gurdon, J. B., Dyson, S. and St. Johnston, D. (1998). Cells' perception of position in a concentration gradient. *Cell* **95**, 159-162

Halpern, M. E., Thisse, C., Ho., R. K., Thisse, B., Riggleman, B., Trevarrow, B., Weinberg, E. S., Postlethwait, J. H. and Kimmel, C. B. (1995). Cell-autonomous shift from axial to paraxial mesodermal development in zebrafish floating head mutants. *Development* **121**, 4257-4264

Harland, R. and Gerhart, J. (1997). Formation and function of Spemann's organizer. *Annu. Rev. Cell Dev. Biol.* **13**, 611-667

Jacob, M., Jacob, H. J., Wachtler, F. and Christ, B. (1984). Ontogeny of avian extrinsic ocular muscles. I. A light- and electron-microscopic study. *Cell Tissue Res* **237**, 549-557

Jones, C. M., Kuehn, M. R., Hogan, B. L. M., Smith, J. C. and Wright, C. V. E. (1995). Nodal-related signals induce axial mesoderm and dorsalize mesoderm during gastrulation. *Development* **121**, 3651-3662

Jones, C. M., Armes, N. and Smith, J. C. (1996). Signalling by TGF-β family members: short-range effects of Xnr-2 and BMP-4 contrast with the long-range effects of activin. *Current Biol.* **6**, 1468-1475

Joseph, E. M. and Melton, D. A. (1997). Xnr4: a Xenopus nodal-related gene expressed in the Spemann organizer. *Dev. Biol.* **184**, 367-372

Jowett, T. and Yan, Y.-L. (1996). Double fluorescent in situ hybridization to zebrafish embryos. *Trends Genet.* **12**, 387-389

Keller, R. E. (1976). Vital dye mapping of the gastrula and neurula of Xenopus laevis. II. Prospective areas and morphogenetic movements of the deep layer. *Dev. Biol.* **51**, 118-137

Kimmel, C. B., Warga, R. M. and Schilling, T.F. (1990). Origin and organization of the zebrafish fate map. *Development* **108**, 581-594

Kimmel, C. B., Ballard, W. W., Kimmel, S. R., Ullmann, B. and Schilling, T. F. (1995). Stages of embryonic development of the zebrafish. *Dev. Dynamics* **203**, 253-310

Kozlowski, D. J., Murakami, T., Ho, R. K. and Weinberg, E. S. (1997). Regional cell movement and tissue patterning in the zebrafish embryo revealed by fate mapping with caged fluorescein. *Biochem. Cell Biol.* **75**, 551-562

Lustig, K. D., Kroll, K., Sun, E., Ramos, R., Elmendorf, H. and Kirschner, M. W. (1996). A *Xenopus* nodal-related gene that acts in synergy with noggin to induce complete secondary axis and notochord formation. *Development* **122**, 3275-3282

Marshall, C. J. (1995). Specificity of receptor tyrosine kinase signaling: transient versus sustained extracellular signal-regulated kinase activation. *Cell* **80**, 179-185

Matzuk, M. M., Kumar, T. R., Vassalli, A., Bickenback, J. R., Roop, D. R., Jaenisch, R. and Bradley, A. (1995). Functional analysis of activins during mammalian development. *Nature* **374**, 354-356

McDowell, N., Zorn, A. M., Crease, D. J. and Gurdon, J. B. (1997). Activin has direct long-range signalling activity and can form a concentration gradient by diffusion. *Curr. Biol.* **7**, 671-681

Melby, A. E., Warga, R. M. and Kimmel, C. B. (1996). Specification of cell fates at the dorsal margin of the zebrafish gastrula. *Development* **122**, 2225-2237

Meno, C., Gritsman, K., Ohishi, S., Ohfuji, Y., Heckscher, E., Mochida, K., Shimono, A., Kondoh, H., Talbot, W. S., Robertson, E. J., Schier, A. F. and Hamada, H. (1999). Mouse Lefty2 and Zebrafish Antivin are feedback inhibitors of Nodal signaling during vertebrate gastrulation. *Molec. Cell* **4**, 287-298

Niehrs, C. Keller, R., Cho, K. W. and DeRobertis, E. M. (1993). The homeobox gene goosecoid controls cell migration in Xenopus embryos. *Cell* **72**, 491-503

Nomura, M. and Li, E. (1998). Smad2 role in mesoderm formation, left-right patterning and craniofacial development. *Nature* **393**, 786-790

Oh, S. P. and Li, E. (1997). The signaling pathway mediated by the type IIB activin receptor controls axial patterning and lateral asymmetry in the mouse. *Genes Dev.* **11**, 1812-1826

Osada, S. I. and Wright, C.V. (1999). Xenopus nodal-related signaling is essential for mesendodermal patterning during early embryogenesis. *Development* **126**, 3229-3240

Piccolo, S., Agius, E., Leyns, L., Bhattacharyya, S., Grunz, H., Bouwmeester, T. and DeRobertis E. M. (1999). The head inducer Cerberus is a multifunctional antagonist of Nodal, BMP and Wnt signals. *Nature* **397**, 707-710

Rebagliati, M. R., Toyama, R., Fricke, C., Haffter, P. and Dawid, I. B. (1998a). Zebrafish nodal-related genes are implicated in axial patterning and establishing left-right asymmetry. *Dev. Biol.* **199**, 261-272

Rebagliati, M. R., Toyama, R., Haffter, P. and Dawid, I. B. (1998b). cyclops encodes a nodal-related factor involved in midline signaling. *Proc. Natl. Acad. Sci. USA* **95**, 9932-7

Rodaway, A., Takeda, H., Koshida, S., Broadbent, J., Price, B., Smith, J. C., Patient, R. and Holder, N. (1999). Induction of the mesendoderm in the zebrafish germ ring by yolk cell-derived TGF-β family signals and discrimination of mesoderm and endoderm by FGF. *Development* **126**, 3067-3078

Sampath, K., Rubinstein, A. L., Cheng, A. M., Liang, J. O., Fekany, K., Solnica-Krezel, L., Korzh, V., Halpern, M. E. and Wright, C. V. (1998). Induction of the zebrafish ventral brain and floorplate requires cyclops/nodal signaling. *Nature* **395**, 185-189

Schier, A. F., Neuhauss, A. F. K., Helde, A., Talbot, W. S. and Driever, W. (1997). The *one-eyed pinhead* gene functions in mesoderm and endoderm formation in zebrafish and interacts with *no tail*. *Development* **124**, 327-342

Schier, A. F. and Talbot, W. S. (1998). The zebrafish organizer. *Curr. Opin. Gen. Dev.* **8**, 464-471

Schier, A. F. and Shen, M. M. (2000). Nodal signaling in vertebrate development. *Nature*, in press

Schulte-Merker, S., Smith, J. C. and Dale, L. (1994). Effects of truncated activin and FGF receptors and of follistatin on the inducing activities of BVg1 and activin: does activin play a role in mesoderm induction? *EMBO J.* **13**, 3533-3541

Serbedzija, G. N., Chen, J. N. and Fishman, M. C. (1998). Regulation in the heart field of zebrafish. *Development* **125**, 1095-1101

Shih, J. and Fraser, S. E. (1995). Distribution of tissue progenitors within the shield region of the zebrafish gastrula. *Development* **121**, 2755-2765

Shih, J. and Fraser, S. E. (1996). Characterizing the zebrafish organizer: microsurgical analysis at the early-shield stage. *Development* **122**, 1313-22

Song, J., Oh, S. P., Schrewe, H., Nomura, M., Lei, H., Okano, M., Gridley, T. and Li, E. The type II activin receptors are essential for egg cylinder growth, gastrulation, and rostral head development in mice. (1999). *Dev. Biol.* **213**, 157-169

Spemann, H. and Mangold, H. (1924). Ueber die Induktion von Embryoanalangen durch Inplantation artfremder Organisatoren. *Wilhelm Roux Arch. EntwMech. Org.* **100**, 599-638

Stachel, S. E., Grunwald, D. J. and Myers, P. Z. (1993). Lithium perturbation and *goosecoid* expression identify a dorsal specification pathway in the pregastrula zebrafish. *Development* **117**, 1261-1274

Strähle, U., Jesuthasan, S., Blader, P., Garcia-Villalba, P., Hatta, K. and Ingham, P. W. (1997). one-eyed pinhead is required for development of the ventral midline of the zebrafish (Danio rerio) neural tube. *Genes and Function* **1**, 131-148

Talbot, W. S., Trevarrow, B., Halpern, M. E., Melby, A. E., Farr, G., Postlethwait, J. H., Jowett, T., Kimmel, C. B. and Kimelman, D. (1995). A homeobox gene essential for zebrafish notochord development. *Nature* **378**, 150-157

Thisse, C., Thisse, B., Halpern, M. E. and Postlethwait, J. H. (1994). Goosecoid expression in neurectoderm and mesendoderm is disrupted in zebrafish cyclops gastrulas. *Dev. Biol.* **164**, 420-9

Thisse, C. and Thisse, B. (1999). Antivin, a novel and divergent member of the TGFbeta superfamily, negatively regulates mesoderm induction. *Development* **126**, 229-240

Vincent, J. P. and O'Farrell, J. P. (1992). The state of engrailed expression is not clonally transmitted during early *Drosophila* development. *Cell* **68**, 923-931

Vodicka, M. A. and Gerhart, J. C. (1995). Blastomere derivation and domains of gene expression in the Spemann Organizer of *Xenopus laevis*. *Development* **121**, 3505-3518

von Dassow, G., Schmidt, J. E. and Kimelman, D. (1993). Induction of the *Xenopus* organizer: expression and regulation of Xnot, a novel FGF and activin-regulated homeobox gene. *Genes Dev.* **7**, 355-66

Wachtler, F., Jacob, H. J., Jacob, M. and Christ, B. (1984). The extrinsic ocular muscles in birds are derived from the prechordal plate. *Naturwissenschaften* **71**, 379-80

Waldrip, W. R., Bikoff, E. K., Hoodless, P. A., Wrana, J. L. and Robertson, E. J. (1998). Smad2 signaling in extraembryonic tissues determines anterior-posterior polarity of the early mouse embryo. *Cell* **92**, 797-808

Warga, R. M. and Nusslein-Volhard, C. (1999). Origin and development of the zebrafish endoderm. *Development* **126**, 827-838

Weinstein, M., Yang, X., Li, C., Xu, X, Gotay, J. and Deng, C. X. (1998). Failure of egg cylinder elongation and mesoderm induction in mouse embryos lacking the tumor suppressor smad2. *Proc. Natl. Acad. Sci. USA* **95**, 9378-9383

Whitman, M. (1998). Smads and early developmental signaling by the TGFbeta superfamily. *Genes Dev.* **12**, 2445-2462

Xu, Q., Holder, N., Patient, R. and Wilson, S.W. (1994). Spatially regulated expression of three receptor tyrosine kinase genes during gastrulation in zebrafish. *Development* **120**, 287-299 (1994)

Yan, Y-T., Gritsman, K., Ding, J., Burdine, R. D., Corrales, J., Price, S. M., Talbot, W. S., Schier, A. F. and Shen, M. M. (1999). Conserved requirement for EGF-CFC genes in vertebrate left-right axis formation. *Genes Dev.* 13, 2527-2537

Yasuo, H. and Lemaire, P. (1999). A two-step model for the fate determination of presumptive endodermal blastomeres in Xenopus embryos. *Current Biol.* **9**, 869-879

Zhang, J., Talbot, W. S. and Schier, A. F. (1998). Positional cloning identifies zebrafish one-eyed pinhead as a permissive EGF-related ligand required during gastrulation. *Cell* **92**,241-251

Zhou, X., Sasaki, H., Lowe, L., Hogan, B. L. and Kuehn, M. R. (1993). Nodal is a novel TGF-beta-like gene expressed in the mouse node during gastrulation. *Nature* **361**, 543-547

Zoltiewics, J. S. and Gerhart, J. C. (1997). The Spemann Organizer of Xenopus is patterned along its anteroposterior axis at the earliest gastrula stage. *Dev. Biol.* **192**, 482-491

Zorn, A. M., Butler, K. and Gurdon, J. B. (1999). Anterior endomesoderm specification in Xenopus by Wnt/beta-catenin and TGF-beta signalling pathways. *Dev. Biol.* **209,** 282-97